Direct AFM Observation of Crystal Twisting and Organization in Banded Spherulites of Chiral Poly(3-hydroxybutyrate-*co*-3-hydroxyhexanoate)

Jun Xu, Bao-Hua Guo, and Zeng-Min Zhang

Institute of Polymer Science & Engineering, Department of Chemical Engineering, School of Materials Science and Technology, Tsinghua University, Beijing 100084, China

Jian-Jun Zhou, Yong Jiang, Shouke Yan, and Lin Li*

State Key Laboratory of Polymer Physics and Chemistry, Institute of Chemistry, Chinese Academy of Sciences, Beijing 100080, China

Qiong Wu and Guo-Qiang Chen

Department of Biological Sciences & Biotechnology, Tsinghua University, Beijing 100084, China

Jerold M. Schultz

Department of Chemical Engineering, University of Delaware, Newark, Delaware 19716

Received January 12, 2004; Revised Manuscript Received March 26, 2004

ABSTRACT: Real-time atomic force microscopy observation was carried out during crystallization in thin films of chiral poly(R-3-hydroxybutyrate-*co*-R-3-hydroxyhexanoate) copolymer, and the development details of single lamellae in the banded spherulites are revealed for the first time. The lamellae exhibit complicated growth behaviors: twisting, bending, backward growth, and branching. The lamellae continuously twist to show alternating edge-on and flat-on views along the radii of the spherulites. Giant screw dislocations bring forth to the birth of new lamellae. Interaction between the leading and trailing lamellae contributes to cooperative stacking of the twisting crystals. The lamellae twist before screw dislocations appear, demonstrating that screw dislocations are not causal of twisting. All the observed twisting occurs in the right-handed sense, likely resulting from the chirality of the crystal structure. Increased crystallization temperature results in decreased magnitude of lamellar twisting and bending. Models for morphological development are discussed in the context of these observations.

Introduction

Regularly twisted crystals have been often found in biological and macromolecular systems. For synthetic polymers, the twisting of crystals is a general feature of banded spherulites, which show alternative bright and dark rings under the polarized light microscope.[1] In these cases, the axis about which twisting occurs is in all cases at a large angle (approaching 90°) to the chain axis. Regularly twisted crystals are found for materials composed of either chiral or nonchiral molecules. In both cases, crystals in a given area are generally found to twist in the same direction. For such twisted crystals, there are two major questions for which there is as yet no generally accepted answer: (1) how does the lamellar twisting develop, and (2) what causes twisting and directs the sense (the handedness) of the twist? (The driving force and the director may be identical, but this is not a priori necessary.) Regarding the director of twisting, this is in some cases determined by the chirality of the chain,[2,3] but this, of course, cannot be determined for systems of nonchiral molecules.

The driving force for twisting relates to the energetic motive force that makes the crystal twist, despite the concomitant increase in the elastic strain energy of the crystal. Several fundamentally different models have been proposed to explain the driving force for twisting. Keith and Padden attributed banding in polymer spherulites to the twisting of lamellae caused by the significantly different overcrowding in opposite fold surfaces as a consequence of a growth asymmetry introduced by already extant chain tilt.[4] Bassett claimed that it is reordering of fold surfaces after the growth of crystal lamellae, which initially have no chain tilt that causes S-bending and "drives" banding.[5] Bassett and co-workers suggested that pressure from cilia trapped between the faces of adjacent lamellae, near giant screw dislocations, plays a major role.[6] Schultz proposed that lamellar twisting occurs in order to avoid compositional or stress fields in the melt near the crystallization front.[7] Both Bassett[5,6] and Schultz (in an earlier work)[8] have proposed that twisting may be caused or implemented by queues of giant screw dislocations of the same hand. None of these models[4−8] require chirality of the molecule, nor do they intrinsically specify the sense of the twisting. Singfield suggested that both the driving force and the director of banding are associated with a stereoselective mechanism or asymmetry operating at the growth front during isothermal crystallization.[9] Considering the special case in which the axis of twisting is identical with the molecular axis, Turner et al. showed that the torque exerted by the chain chirality in a biological macromolecule is quantitatively sufficient to cause the observed chain twisting.[3]

Although there are significant differences in explaining the origin of banding in polymer spherulites, it is

* To whom correspondence should be addressed: e-mail lilin@iccas.ac.cn; Ph 0086-10-8261-9830; Fax 0086-10-82619830.

10.1021/ma0499122 CCC: $27.50
Published on Web 04/28/2004

well accepted that banding in polymer spherulites can be attributed to a twisting of crystallographic orientation about radii.[1,2,4−9]

In the past half a century, to reveal the banding mechanism, many investigations on the characterization of lamellar morphology in banded spherulites have been carried out, using scanning electron microscopy (SEM), transmission electron microscopy (TEM), microfocus wide-angle X-ray diffraction (WAXD), and atomic force microscopy (AFM). Different lamellar morphologies have been reported, such as twisted lamellar stacks, consecutive isochiral spiral terraces, individual C- and S-profiled lamellae, and suddenly changed lamellar orientation.[10] However, up to now, how these twisting crystals develop during growth and organize in a spherulite to form regular bands is still somewhat unclear. In this article, we report the in situ and in real time AFM observations demonstrating the process and details of twisting of single lamellae during spherulitic growth from the melt. The work is performed using poly(R-3-hydroxybutyrate-*co*-R-3-hydroxyhexanoate) (PHB-*co*-HHx). It has been reported that in PHB-*co*-HHx random copolymers, only HB units can crystallize, with HHx units excluded from the crystal lattice as defects.[11] Thus, the PHB-*co*-HHx copolymer is attractive for study on lamellar twisting since its crystallization rate can be adjusted by varying the composition.

Experimental Section

Poly(R-3-hydroxybutyrate-*co*-R-3-hydroxyhexanoate) random copolymer (PHB-*co*-HHx) with 17 mol % HHx content was fractionated according to Inoue's method[12] from the as-produced copolymer biosynthesized by *Aeromonas hydrophila* 4AK4.[13] The glass transition temperature, melting point, and number-average molecular weight of this polymer were measured to be −2.1 °C, 100.1 °C, and 3.17×10^5 g/mol, respectively.

PHB-*co*-HHx powder was melted between two clean glass slides at 180 °C for 3 min, then quickly transferred onto a hot bench preset at 45 °C, and crystallized for 16 h. The spherulitic morphology was observed under a polarized optical microscope (BH-2, Olympus) coupled with a computer-controlled CCD camera (Sanyo Electric Co. Ltd.).

Thin films of PHB-*co*-HHx about 100 nm were prepared via spin-coating 0.5 wt % chloroform solution onto a freshly cleaved mica surface, and the crystallization processes at room temperature and higher temperatures were observed directly under tapping-mode AFM using a Nanoscope III MultiMode AFM (Digital Instruments) equipped with a high-temperature heater accessory (Digital Instruments). Both height and phase images were recorded simultaneously. Typical values for the set-point amplitude ratio (r_{sp} is defined as the ratio of the cantilever's oscillating amplitude to its freely oscillating amplitude) were 0.7−0.9. The amplitude of the freely oscillating cantilever was approximately 40 nm. TESP tips with a resonance frequency of approximately 300 kHz and a spring constant of about 30 N/m were used. The experimental details of high-temperature AFM can be found elsewhere.[14] The images shown here were subjected to first-order plane-fitting and first-order flattening procedures to compensate for the sample tilt.

Results

When crystallized from the melt at 45 °C, PHB-*co*-HHx forms banded spherulites with band spacing of approximately 1 μm, as presented in Figure 1. The spherulites exhibit both Maltese cross and concentric extinction bands when observed under the polarized optical microscope (POM), as shown in Figure 1a. Banded structures of the spherulite can also be observed

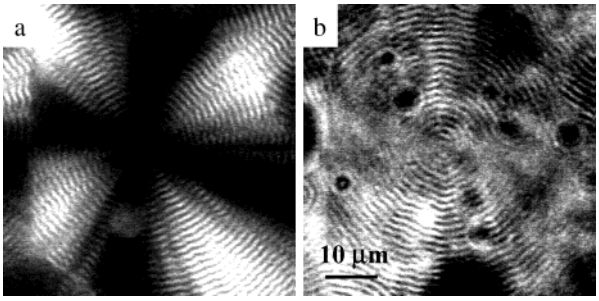

Figure 1. Optical microscopic photos of PHB-*co*-HHx banded spherulites crystallized at 45 °C: (a) polarized light; (b) phase contrast.

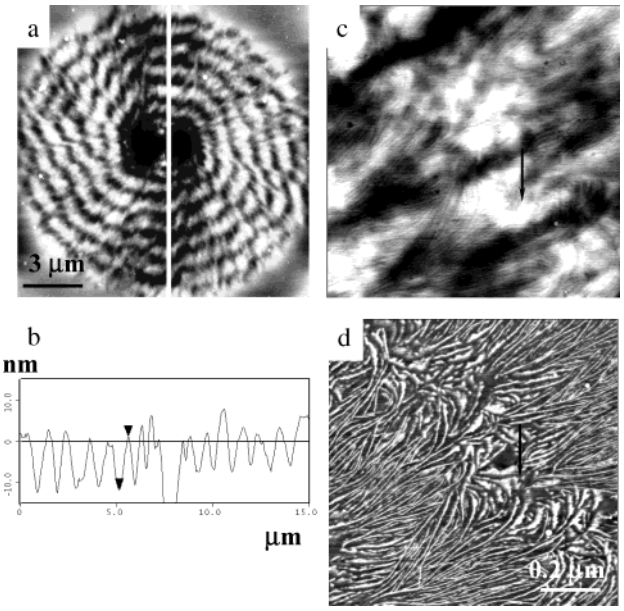

Figure 2. AFM images showing topography of PHB-*co*-HHx banded spherulites crystallized at 45 °C: (a) height image showing the overall morphology; (b) cross section of the spherulite along the line shown in (a); (c) height image showing some ridges and valleys; (d) phase image showing the lamellar morphology in the same region as (c).

with the phase contrast mode, as shown in Figure 1b. The bands in the phase contrast mode reveal the variation of refractive index along the radial direction of the spherulite. Figure 2a presents an AFM height image to show the surface topography of a banded spherulite isothermally crystallized at 45 °C. The banded structures observed by AFM are similar to the alternate bright and dark bands observed by POM. The AFM cross-section analysis shows that the average band spacing is the same as that observed by POM, and the average height of undulation is around 10 nm, as shown in Figure 2b. Figure 2c,d presents the high-magnification AFM height and phase images showing the twisting region of the banded spherulite. The bright area indicates the ridge area of the surface as indicated by an arrow in the height image (cf. Figure 2c), which, in turn, is seen in the phase image (Figure 2d) to consist of flat-on lamellae. Correspondingly, the valley area is filled by edge-on lamellae. It is noteworthy that the lamellar crystals appear to be significantly bent, being best directed toward the growth direction at the valley area of the spherulite surface. The directions of twisting and of bending remain fixed over the field of view. Figure 3 presents a series of AFM height images showing how the banded structures are formed during the growth of

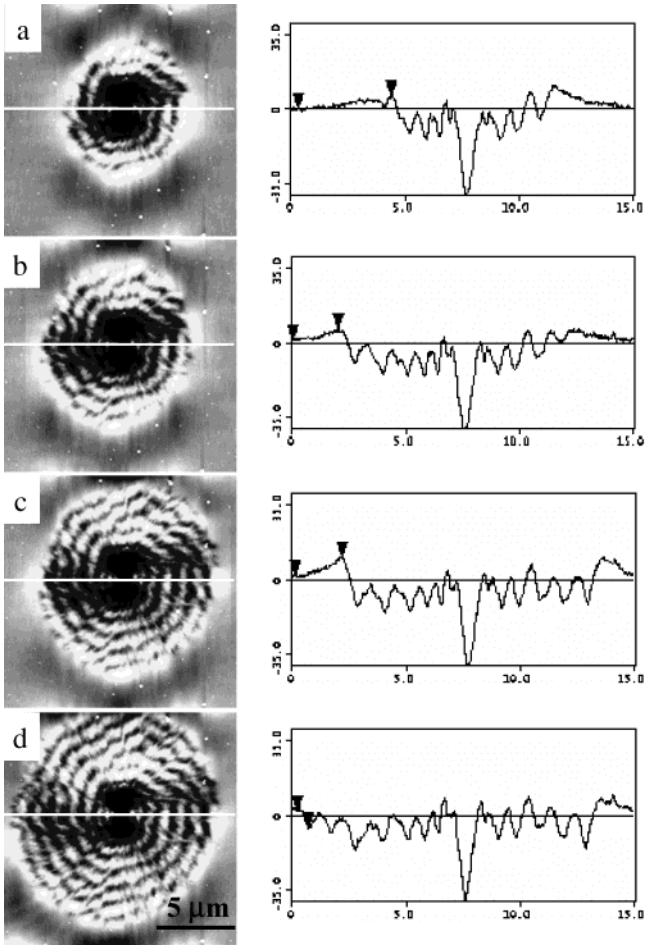

Figure 3. AFM height images and cross section profiles showing the growth of a PHB-*co*-HHx banded spherulite at 45 °C.

a PHB-*co*-HHx spherulite. The left column shows the consecutive height images, and the right presents the corresponding cross-section analysis. Figure 3 shows a growing spherulite with two eyelets at the center, resulting from continuous branching and splaying of lamellae from the initial sheaf structure. The successive images clearly resemble the optical micrographs as they display a sharply defined growth front. Both the height images and the cross sections show that the melt is thicker near the growing front than further away. This effect is likely due to material transportation from the rubbery liquid to the growing front.

Consecutive high-magnification phase images obtained in situ at room temperature show the lamellar growth process in a banded spherulite, as revealed in Figure 4. Figure 4a shows some leading edge-on lamellae protruding into the melt, as indicated by the arrow A. The formation of an edge-on lamella is the result of twisting of an existing flat-on lamella. After growing to a certain length, it is observed that the edge-on lamellae twist again and lamellae with tilt orientations can be seen, as indicated by the arrow B in Figure 4b. After further growth, the lamellae twist to the flat-on orientation, as shown by the arrow C in Figure 4c. The twisting of the flat-on lamellae to show the traces of the edge-on lamellae is indicated by the arrow D in Figure 4c. In Figure 4d, the edge-on lamellae further grow forward. However, because of the dense lamellar packing and the relative fast growth rate, the details of lamellar twisting cannot be distinguished.

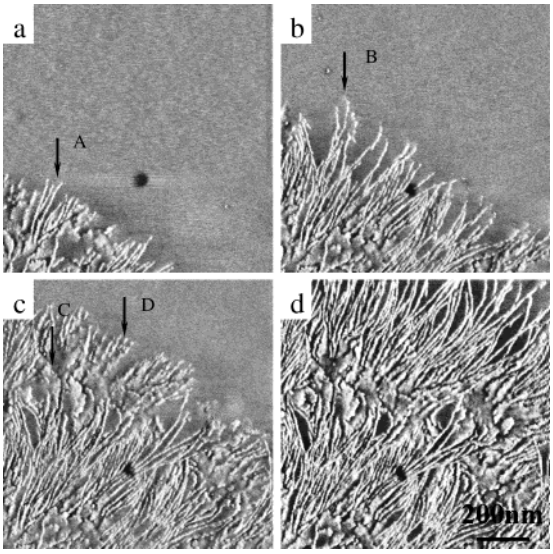

Figure 4. High-resolution in situ AFM phase images showing lamellar growth in PHB-*co*-HHx banded spherulites. The time interval between the two consecutive images is 5 min.

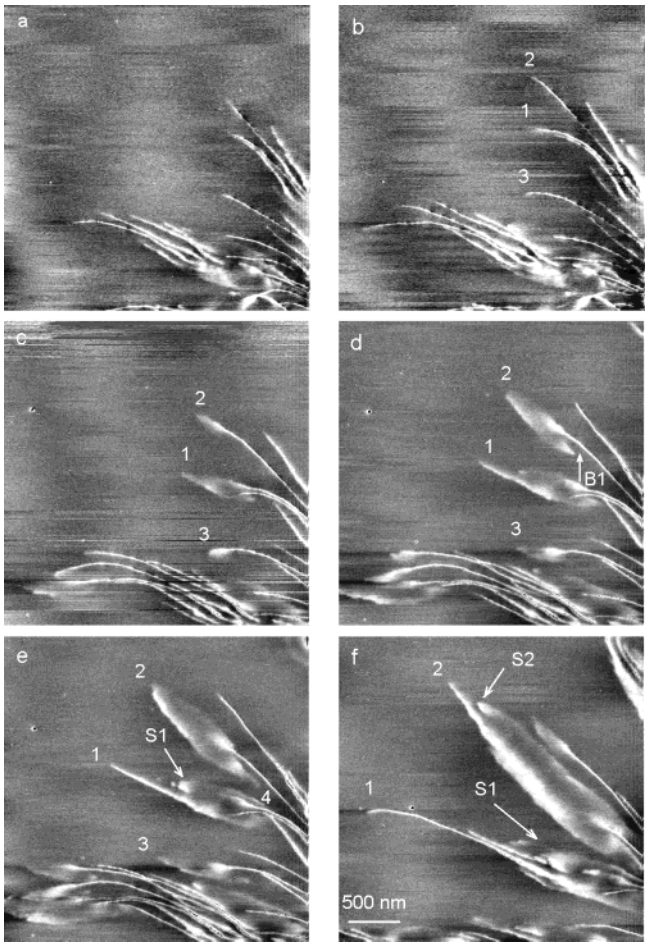

Figure 5. Real-time AFM phase images showing lamellar twisting process at 75 °C. The images in (b), (c), (d), (e), and (f) correspond to elapsed time of 6, 12, 18, 24, and 36 min, respectively, with respect to the first image.

With increasing crystallization temperature, the twisting process becomes even clearer. Figure 5 presents a series of high-resolution AFM phase images obtained at 75 °C, showing how a single lamella changes its orientation during growth. The scan region has been

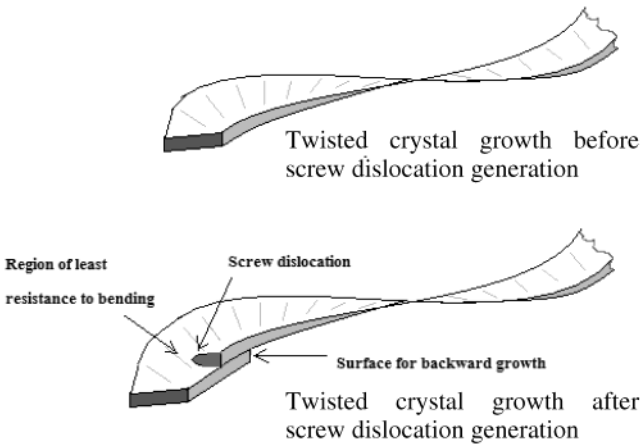

Figure 6. Model of the effects of a giant screw dislocation on crystal morphology: access to backward growth and reduced cross section for twisting.

shifted to follow the growth front of the spherulite. Figure 5a presents some leading edge-on lamellae protruding into the melt. After the leading edge-on lamellae grow to a length of about 2 μm, as labeled by 1, 2, and 3, they bend counterclockwise toward the tangential direction, as shown in Figure 5b. Moreover, they twist to become flat-on lamellae, which is clearly seen in lamellae 2 and 3. They twist further to show a tilted view at the tip in Figure 5c and then grow forward and twist further to reveal a flat-on view in Figure 5d. The flat-on lamellae appear with a lozenge-shaped profile and grow both forward and backward, as indicated by an arrow B1 in Figure 5d. The degree (pitch) of the twist is amplified in such regions. It is difficult to envision how backward growth can occur unless a screw dislocation provides a new back-directed growth surface. This situation is sketched in Figure 6. Backward growth and twisting of the flat-on lamella 2 lead to the birth of a new edge-on lamella 4, as shown in Figure 5e. Because of the depletion of the available melt, growth in the backward direction becomes slow and finally stopped. Figure 5d−f shows the process of a flat-on lamella twisting during growth into the edge-on orientation. When a flat-on lamella, e.g., lamella 1, grows to a certain length, about 1.5 μm, screw dislocations appear behind the growth tip, resulting in the birth of new lamellae at both sides of the leading lamella, indicated by arrows S1 and S2. Further growth and twisting of these lamellae lead to their orientation changes likewise from flat-on to edge-on views, as seen in Figure 5e,f. The observations in Figure 5 sequence also show that the twisting becomes accentuated in the vicinity of screw dislocations. Conceptually, this accentuated twisting near a screw dislocation is expected because of the effectively decreased cross section, as indicated schematically in Figure 6. Continuous growth and branching of lamellae result in filling of the interlamellar regions. These real-time AFM observations demonstrate that twisting leads directly and continuously to the alternating edge-on and flat-on orientations. This is the first time that real-time twisting of the individual lamellae in banded spherulites has been revealed at such high resolution.

The lengths of lamellae 1 and 2 in Figure 5 are plotted vs the observation time in Figure 7. The open and closed data markers indicate the growth profile of lamellae 1 and 2, respectively. The average growth rates of the lamellae in the radial direction are 0.9 nm/s for lamella

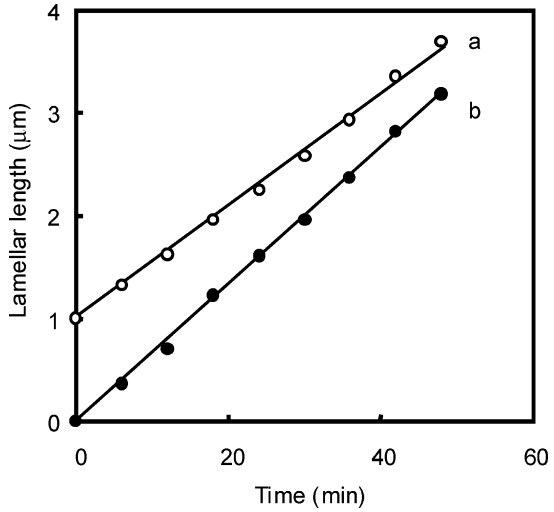

Figure 7. Crystal length vs time for two different crystals growing at 75 °C. The growth velocities of lamella 1 (a) and lamella 2 (b) are 0.9 and 1.1 nm/s, respectively.

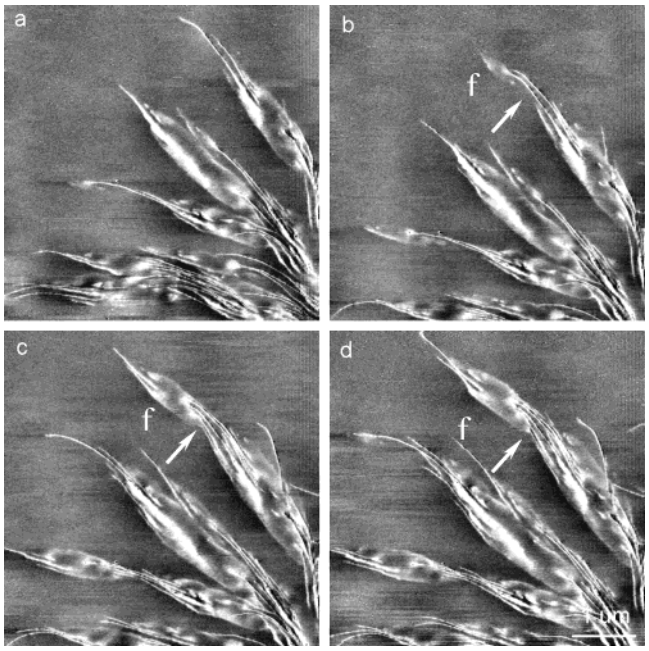

Figure 8. Real-time AFM phase images showing lamellar packing in the spherulite at 75 °C. The images in (b), (c), and (d) correspond to elapsed time of 6, 18, and 24 min, respectively, with respect to the first image.

1 and 1.1 nm/s for lamella 2, respectively, demonstrating a constant growth rate of the twisting lamellae.

Further understanding of the organization of the lamellae of different orientations can be obtained from the sequence shown in Figure 8 for crystallization at 75 °C. One again observes continuous twisting of lamellae, with the sense of the twisting everywhere the same. Again, while the twisting is continuous, it appears amplified near screw dislocations. From Figure 8b−d, the flat-on lamella (marked f) at the up-right corner widens. When the trailing edge-on lamellae impinge with the leading flat-on lamella, the net effect is that the final morphology can appear as a stack of crystals, forming a twisted line of stacks of the same sense of twisting but exhibiting sudden changes of orientation between the stacks when observed in mature spherulites. The lamellar morphology in Figure 8 shows some similarity to the twist and splay of lamellae in poly-

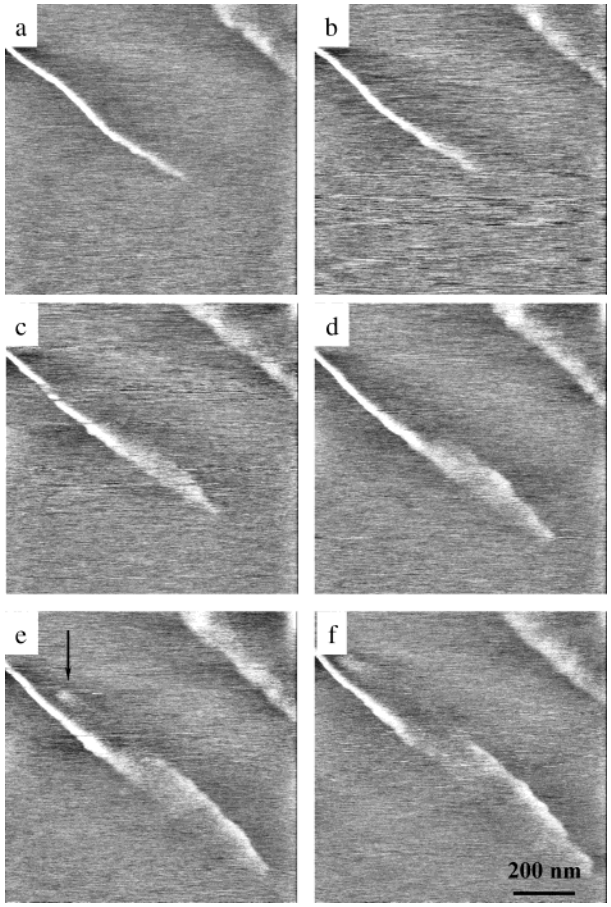

Figure 9. Real-time AFM phase images showing lamellar twisting from edge-on to flat-on at 85 °C. The time intervals between two consecutive images are 6 min.

(vinylidene fluoride) banded spherulites grown from poly(vinylidene fluoride)/poly(ethyl acrylate) blends.[15] The splay was proposed to result from periodic stress buildup and release. However, the growth segments in the twisting-splay motif reported by Briber and Khoury are mainly macrobranches consisting of stacked interleaving lamellae. Our real-time observations on the lamellar level demonstrate that the splay observed here results from interleaving of the edge-on lamellae grown from a mother lamella via screw dislocations.

When the sample was crystallized at 85 °C, the growth rate of the lamellae decreased further to 0.5 nm/s, which makes the twisting process more clearly visible. Figure 9 shows the twisting process of the leading lamellae from edge-on to flat-on view. The backward growing lamella first grows below the film, and it is observed until it grows into the surface of the film, as indicated by an arrow in Figure 9e. It is demonstrated that the lamella changes orientation continuously to form a helical twisting profile.

The effects of crystallization temperature on the pitch of twisting and the radius of bending curvature are plotted in Figure 10. The pitch of crystal twisting, or band spacing of the spherulites, increases with crystallization temperature, in accordance with the literature. The radius of curvature also increases with crystallization temperature and indeed shows the same quantitative trend, with a constant multiplier between the two. Consequently, it would appear that the bending force has the same origin as the twisting force. Further, it is observed (not described here) that the average distance

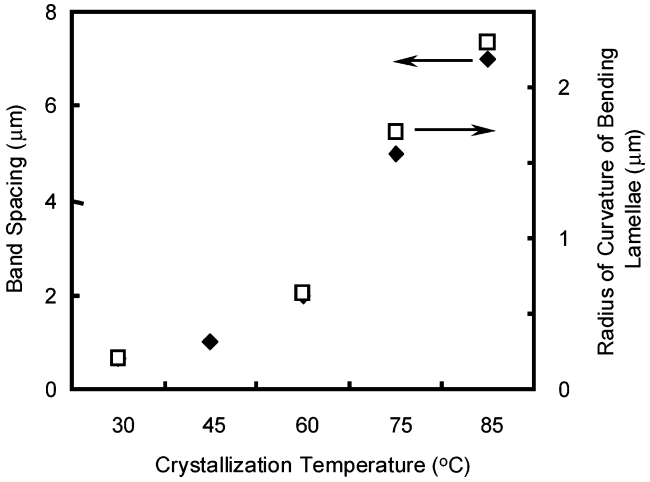

Figure 10. Dependence of the band spacing and the radius of bending curvature on the crystallization temperature. The closed data marker indicates the band spacing, and the open marker represents the radius of bending curvature of lamellae.

between two neighboring screw dislocations also increases with crystallization temperature, an effect that is probably correlated with the decreased shear stress due to a larger pitch of twisting.

Discussion

We discuss here two topics: the implications of the giant screw dislocations and the mechanism responsible for crystal twisting.

The observations described here have shown three properties of giant screw dislocations. First, they are not causal for crystal twisting. Crystals are observed to twist far from the position of any screw dislocation. At least for the material studied here, models of twisting which *require* the formation of giant screw dislocations are not valid. Second, twisting is accentuated near giant screw dislocations, probably because of an effective decrease in the cross section.

The ultimate driving force for crystal twisting is still an open question and far beyond the reach of this investigation. There is nothing in the present observations which speaks either for or against Bassett's model, in which twisting is caused by reordering of fold surfaces in flat crystals initially without chain tilt;[5] Keith and Padden's model, in which twisting is caused by the significantly different overcrowding in opposite fold surfaces as a consequence of a growth asymmetry introduced by already extant chain tilt;[4] or Singfield's association of twisting with stereoselective mechanism or asymmetry operating at the growth front.[9] On the other hand, the present observations are not in accordance with models that require screw dislocations to create the twist, for instance the older model of Schultz.[8] In Figure 8, because further growth of the lamellae obscured the twisting details, the final lamellar morphology in the banded spherulite shows the appearance of abrupt change of lamellar orientation. Consequently, the abrupt change of lamellar orientation in the final morphology cannot sufficiently support the hypothesis of noncontinuous twist consisting of short lamellar segments rotated vs each other along the radius by discrete angles.[16] In terms of the present observations, the more recent Bassett model on polyethylene is not applicable to the only right-handed lamellar twist in the chiral polyester spherulite. If the

chain stems in the lamellae were initially normal to the fold surface and reordering led to chain tilt then lamellar twisting, the chain tilt toward both directions should exist, which should result in the lamellar twisting in both directions. In our case, lamellar twisting may result from several reasons: self-generated compositional or stress field, asymmetric surface stress, etc.

Why all the observed lamellar crystals twist in the right-handed sense is still unclear and deserves further investigation. The fixed twisting sense likely relates to the chirality in the molecular chains or high structural levels.

Conclusion

Real-time AFM observation of twisting of single lamellae and their organization in the banded spherulite is reported for the first time in chiral PHB-*co*-HHx, which provides rich information on the growth of the lamellar crystals: twisting, bending, backward growth, screw dislocations, etc. The lamellae change their orientation via continuous twisting, whereby the giant screw dislocations on the twisting crystals lead to lamellar branching to fill the space. Crystals are observed to twist far from the position of any screw dislocation, which demonstrates that screw dislocations are not necessary to cause lamellar twisting in the banded spherulites. A special mechanism resulting in cooperative organization of the twisting crystals in the spherulites is revealed: The leading edge-on lamellae twist to flat-on view first, widening of the new flat-on lamellae retard growth of the trailing edge-on lamellae; screw dislocations on the twisting crystals give birth to a stack of lamellae with almost the same orientation.

Acknowledgment. This work was supported by the Outstanding Youth Fund and National Science Foundation of China (Grants 20174049, 50273044, and 2013-1160730). Dr. Jun Xu is grateful to the financial support from the Fundamental Research Fund of Tsinghua University (Grant Jc2003037).

References and Notes

(1) (a) Keller, A. *J. Polym. Sci.* **1955**, *17*, 291−308. (b) Keith, H. D.; Padden, F. J., Jr. *J. Polym. Sci.* **1959**, *39*, 101−122. (c) Price, F. P. *J. Polym. Sci.* **1959**, *39*, 139−150. (d) Keller, A. *J. Polym. Sci.* **1959**, *39*, 151−173. (e) Fujiwara, Y. *J. Appl. Polym. Sci.* **1960**, *4*, 10−15.

(2) (a) Chothia, C. *J. Mol. Biol.* **1973**, *75*, 295−302. (b) Lotz, B.; Gonthier-Vassal, A.; Brack, A.; Magoshi, J. *J. Mol. Biol.* **1982**, *156*, 345−357. (c) Wilson-Kubalek, E. M.; Brown, R. E.; Celia, H.; Milligan, R. A. *Proc. Natl. Acad. Sci. U.S.A.* **1998**, *95*, 8040−8045. (d) Dogic, Z.; Fraden, S. *Philos. Trans. R. Soc. London A* **2001**, *359*, 997−1015. (e) Li, C. Y.; Cheng, S. Z. D.; Ge, J. J.; Bai, F.; Zhang, J. Z.; Mann, I. K.; Harris, F. W.; Chien, L.-C.; Lotz, B. *Phys. Rev. Lett.* **1999**, *83*, 4558−4561. (f) Kubel, C.; Lawrence, D. P.; Martin, D. C. *Macromolecules* **2001**, *34*, 9053−9058.

(3) Turner, M. S.; Briehl, R. W.; Ferrone, F. A.; Jesophs, R. *Phys. Rev. Lett.* **2003**, *90*, 128103.

(4) (a) Keith, H. D.; Padden, F. J., Jr. *Polymer* **1984**, *25*, 28−42. (b) Keith, H. D.; Padden, F. J., Jr.; Lotz, B.; Wittmann, J. C. *Macromolecules* **1989**, *22*, 2230−2238. (c) Keith, H. D.; Padden, F. J., Jr. *Macromolecules* **1996**, *29*, 7776−7786. (d) Keith, H. D.; Chen, W. Y. *Polymer* **2002**, *43*, 6263−6272.

(5) (a) Bassett, D. C. In Dosière, M., Ed.; *Crystallization of Polymers;* Kluwer: Dordrecht, The Netherlands, 1993; p 107. (b) Bassett, D. C. *Philos. Trans. R. Soc. London A* **1994**, *348*, 29−44. (c) Abo el Matty, M. I.; Bassett, D. C. *Polymer* **2001**, *42*, 4957−4963.

(6) (a) Bassett, D. C.; Olley, R. H.; Sutton, S. J.; Vaughan, A. S. *Macromolecules* **1996**, *29*, 1852−1853. (b) Abo el Maaty, M. I.; Hosier, I. L.; Bassett, D. C. *Macromolecules* **1998**, *31*, 153−157.

(7) Schultz, J. M. *Polymer* **2003**, *44*, 433−441.

(8) Schultz, J. M.; Kinloch, D. R. *Polymer* **1969**, *10*, 271−278.

(9) (a) Singfield, K. L.; Brown, G. R. *Macromolecules* **1995**, *28*, 1290−1297. (b) Singfield, K. L.; Klass, J. M.; Brown, G. R. *Macromolecules* **1995**, *28*, 8006−8015. (c) Singfield, K. L.; Hobbs, J. K.; Keller, A. *J. Cryst. Growth* **1998**, *183*, 683−689.

(10) (a) Keller, A.; Sawada, S. *Makromol. Chem.* **1964**, *74*, 190−221. (b) Toda, A.; Arita, T.; Hikosaka, M. *Polymer* **2001**, *42*, 2223−2233. (c) Patel, D.; Bassett, D. C. *Polymer* **2002**, *43*, 3795−3802. (d) Sasaki, S.; Sasaki, Y.; Takahara, A.; Kajiyama, T. *Polymer* **2002**, *43*, 3441−3446. (e) Crämer, K.; Lima, M. F. S.; Magonov, S. N.; Hellmann, E. H.; Jacobs, M.; Hellmann, G. P. *J. Mater. Sci.* **1998**, *33*, 2305−2312.

(11) (a) Doi, Y.; Kitamura, S.; Abe, H. *Macromolecules* **1995**, *28*, 4822−4828. (b) Abe, H.; Doi, Y.; Aoki, H.; Akehata, T. *Macromolecules* **1998**, *31*, 1791−1797.

(12) (a) Watanabe, T.; He, Y.; Fukuchi, T.; Inoue, Y. *Macromol. Biosci.* **2001**, *1*, 75−83. (b) Feng, L. D.; Watanabe, T.; Wang, Y.; Kichise, T.; Fukuchi, T.; Chen, G. Q.; Doi, Y.; Inoue, Y. *Biomacromolecules* **2002**, *3*, 1071−1077.

(13) Chen, G. Q.; Zhang, G.; Park, S. J.; Lee, S. Y. *Appl. Microbiol. Biotechnol.* **2001**, *57*, 50−55.

(14) (a) Jiang, Y.; Jin, X. G.; Han, C. C.; Li, L.; Wang, Y.; Chan, C. M. *Langmuir* **2003**, *19*, 8010−8018. (b) Jiang, Y.; Yan, D. D.; Gao, X.; Han, C. C.; Jin, X. G.; Li, L.; Wang, Y.; Chan, C. M. *Macromolecules* **2003**, *36*, 3652−3655. (c) Schonherr, H.; Bailey, L. E.; Frank, C. W. *Langmuir* **2002**, *18*, 490−498. (d) Ivanov, D. A.; Amalou, Z.; Magonov, S. N. *Macromolecules* **2001**, *34*, 8944−8952. (e) Hobbs, J. K.; Humphris, A. D. L.; Miles, M. J. *Macromolecules* **2001**, *34*, 5508−5519. (f) Godovsky, Yu. K.; Magonov, S. N. *Langmuir* **2000**, *16*, 3549−3552.

(15) Briber, R. M.; Khoury, F. *J. Polym. Sci., Part B: Polym. Phys. Ed.* **1993**, *31*, 1253−1272.

(16) (a) Bassett, D. C.; Hodge, A. M. *Polymer* **1978**, *19*, 469−472. (b) Vaughan, A. S. *J. Mater. Sci.* **1993**, *28*, 1805−1813.

MA0499122